Management of positioning functions in cellular networks for time-sensitive transportation applications

Management of positioning functions in cellular networks for time-sensitive transportation applications

Qirui Liu, *Graduate Student Member, IEEE,* Rongke Liu, *Senior Member, IEEE,* Yang Zhang, *Member, IEEE,* Yanli Yuan, *Member, IEEE,* Zijie Wang, Haolan Yang, Lin Ye, Mohsen Guizani, *Fellow, IEEE,* and John S. Thompson, *Fellow, IEEE*

***Abstract*—Device positioning has generally been recognized as an enabling technology for numerous vehicular applications in intelligent transportation systems (ITS). The downlink time difference of arrival (DL-TDOA) technique in cellular networks requires range information of geographically diverse base stations (BSs) to be measured by user equipment (UE) through the positioning reference signal (PRS). However, inter-cell interference from surrounding BSs can be particularly serious under poor network planning or dense deployments. This may lead to a relatively longer measurement time to locate the UE, causing an unacceptable location update rate to time-sensitive applications. In this case, PRS muting of certain wireless resources has been envisioned as a promising solution to increase the detectability of a weak BS. In this paper, to reduce UE measurement latency while ensuring high location accuracy, we propose a muting strategy managed by positioning functions that utilizes a combination of optimized pseudo-random sequences (CO-PRS) for multiple BSs to coordinate the muting of PRS resources. The original sequence is first truncated according to the muting period, and a modified greedy selection is performed to form a set of control sequences as the muting configurations (MC) with balance and concurrency constraints. Moreover, efficient information exchange can be achieved with the seeds used for regenerating the MC. Extensive simulations demonstrate that the proposed scheme outperforms the conventional random and ideal muting benchmarks in terms of measurement latency by about 30%, especially when dealing with severe near-far problems in cellular networks.**

***Index Terms*—Positioning functions, base stations management, pseudo-random muting, time-sensitive, downlink time difference of arrival (DL-TDOA).**

This work was supported by the Beijing Natural Science Foundation under Grant (L202003) and Shenzhen Fundamental Research Program under Grant (JCYJ20220818103413029). *(Corresponding author: Rongke Liu and Yanli Yuan.)*

Q. Liu, Z. Wang, H. Yang and L. Ye are with the School of Electronic and Information Engineering, and also with Shenyuan Honors College of Beihang University, Beijing 100191, China (e-mail: {qirui_liu, wangmajie, yanghaolan, 19376373}@buaa.edu.cn).

R. Liu is with the School of Electronic and Information Engineering, Beihang University, Beijing 100191 and also with Shenzhen Institute of Beihang University, Shenzhen 518063, China (e-mail: rongke_liu@buaa.edu.cn).

Y. Zhang is with the College of Computer Science and Technology, Nanjing University of Aeronautics and Astronautics, Nanjing 210016, China (e-mail: yangzhang@nuaa.edu.cn).

Y. Yuan is with the Singapore University of Technology and Design, Singapore 487372 (e-mail: yanli_yuan@alumni.sutd.edu.sg).

M. Guizani is with the Machine Learning Department, Mohamed Bin Zayed University of Artificial Intelligence (MBZUAI), Abu Dhabi, UAE (e-mail: mguizani@ieee.org).

J. S. Thompson is with the Institute for Digital Communications, School of Engineering, University of Edinburgh, King's Buildings, Edinburgh, EH9 3JL, U.K. (e-mail: john.thompson@ed.ac.uk).

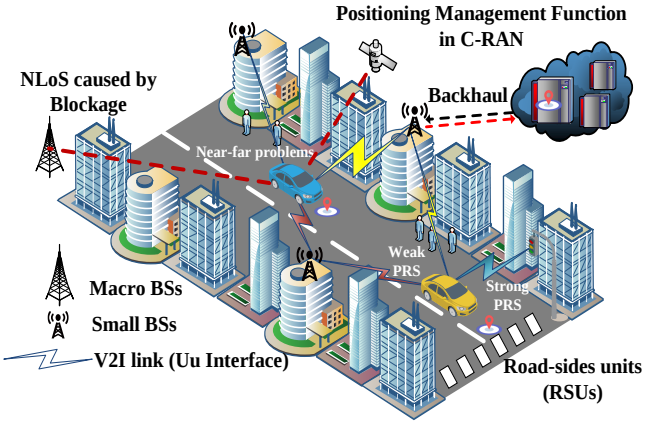

Fig. 1. A typical use case of positioning functions with cellular BSs for time-sensitive transportation applications.

I. Introduction

A. Motivation

POSITIONING services which can reduce latency while ensuring the required accuracy can significantly improve the timeliness of location information, which is vitally important for various dynamic vehicular applications in intelligent transportation systems (ITS), e.g., mobile marketing, logistic tracking, and traffic scheduling [1]–[5].

The widely used Global Navigation Satellite Systems (GNSS) offers an affordable and easily accessible position information as an add-on service to a user equipment (UE). However, satellite-based positioning systems suffer a severe deterioration due to frequent blockage and degradation in dense urban environments [6], [7]. To make matters worse, GNSS jammers and cycle slips in the real time kinematic (RTK) approaches would also inevitably lead to undesirable system outages [8], [9]. Fortunately, the growing ubiquity of cellular vehicle-to-everything (C-V2X) networks can be used to provide self-contained positioning services, such as the downlink time difference of arrival (DL-TDOA) approaches in the Long-Term Evolution (LTE) and fifth generation (5G) standard releases of the Third Generation Partnership Project (3GPP) [10], [11]. The DL-TDOA is a typical range-based UE-assisted positioning method, in which the positioning accuracy will be significantly influenced by the time delay measured by

UE through the positioning reference signals (PRS) transmitted by multiple base stations (BSs) [12], [13]. As shown in Fig. 1, positioning functions in the advanced cellular network architectures, especially the cloud radio access network (C-RAN) [14], [15], will make the implementation of precise positioning more convenient. In particular, dense small cells and road side units (RSU) in urban scenarios generally decrease the distance between the UE and the nearest BSs, which provide abundant measurement information on top of GNSS satellites and conventional macro BSs [16]. By exploiting the ubiquitous vehicle-to-infrastructure (V2I) or even vehicle-to-everything (V2X) communication channels, seamless positioning services are expected to be achieved with the evolution into 5G and beyond [17], [18].

However, inter-cell interference to the received PRS from surrounding BSs can be serious and results in degeneration on ranging accuracy due to poor network planning or dense deployments [19]. This leads to the code phase errors from inadequate cross-correlation results between the received PRS and the local reference signals configured by positioning functions through cellular positioning protocols [13]. Moreover, the UE typically needs range information with at least 4 anchors to estimate its three-dimensional (3D) position using estimation algorithms like the weighted least squares (WLS) [6], [20], and the range error can be increased through poor geometry of the anchors in the location estimation process [21]. Although a higher positioning accuracy can be achieved by averaging the estimation results from multiple received signal units (e.g., a number of subframes containing the PRS), approaches that use more time-frequency resources to acquire more location information will cause a relatively longer measurement delay in the ranging process, thus reducing the position update rate in time-sensitive transportation applications. In this case, muting of PRS managed by positioning functions at specific wireless resources has been proposed to increase both the accuracy and detectability of the PRS from far-away BSs [22], which can then enable optimization of the location accuracy-timeliness trade-off in the ITS [23].

B. Related Works

In order to guarantee a lower end-to-end latency of cellular positioning for time-sensitive transportation applications like intelligent vehicle scheduling, one effective methods is to reduce the latency at the step of implementing range or other geometry-related measurement [24].

Nevertheless, previous work in cellular positioning mainly focuses on the achievable accuracy and methods to improve this. For example, the method in [22] has analyzed the range estimation performance of PRS-based positioning in the scenario of no co-frequency interference, using the evaluation metric of Cramer-Rao lower bound (CRLB) and gives guidance to positioning services in future terrestrial communication networks. New opportunities in cellular positioning like the massive multiple-input-multiple-output (MIMO) also introduce more degree of freedom (DoF) for location and sensing applications [25], [26], and the expression of CRLB has also been derived in [27], [28]. A general-purpose antenna extension solution has been proposed in [29], which can provide extended radio chains of commodity devices for both communication and localization [30]. Besides the design of novel estimation methods as in [6], [31], researches in [32]–[34] have successively proposed a series of deployment strategies for anchor nodes for accurate location estimation in cellular internet-of-things (IoT) networks. These papers mainly assume that the PRS transmitted by each BS is not interfered by other BSs. Practically, the ideal muting strategy is to transmit the PRS sequentially, which is a simple way to ensure high measurement accuracy with almost zero interference. However, in practice, when the number of BSs increases dramatically, the UE measurement latency can be very high and causes a waste of wireless resources [17], [35].

In fact, the interference caused by inappropriate reuse of wireless resources among multiple BS should also be considered for a more practical case, where the accuracy of estimation results will possibly be degraded. Although averaging multiple estimation results from cross-correlation process can bring certain gains against noise and interference, this strategy will also need more measurement time and diminish the timeliness of location information. Henk *et al*. [36] pointed out that if these challenges of interference can be addressed and the BSs can share their coordinates, cellular networks can enable ultra-accurate positioning for dynamic vehicular applications.

The ideal muting idea can be regarded as a simple heuristic interference coordination method by allocating the PRS transmission independently in the time domain. However, the densely deployed BSs have to wait to communicate with UE in turn from the start of the positioning service, which may also cause severe delay on the time to first fix (TTFF) in numerous real time traffic estimation applications [37]. Except for the ideal muting method, several modified muting methods like interference cancellation (IC) [22] and random muting [19] have also been proposed to coordinate PRS transmission of BSs sharing the same resources. Generally speaking, these muting strategies still exhibit certain limitations and inflexibility from a low-latency positioning perspective. The IC technique generally needs to reconstruct the signal from the strongest BS and then subtract it from the received signal, which then obtains a superposition of the signals from the weaker BSs. Nonetheless, the subtraction of strongest signal may induce higher complexity and latency to the UE receiver. Different frequency offsets given by the physical cell identity (PCID) is also allowed from the LTE standard to avoid collisions for up to six neighbor BS [38]. However, this strategy may not be sufficient with poor PCID planning [39]. Furthermore, randomization of PRS muting in [19] designed the muting pattern for each BS in the target area, e.g., using random binary 1/0 sequences with 50% duty cycle to determine the ON/OFF state of PRS transmission over a period of time. Nevertheless, the random method cannot control the concurrent PRS transmission precisely and the corresponding muting pattern would generate a relatively large amount of signaling traffic.

In general, PRS Muting can be regarded as an interference management method for positioning purposes. For communication services in cellular networks, popular methods like

power and channel access allocation [40], [41], task offloading [42] and user association [43] are widely used recently to improve the system utility. However, due to the difference between communication and positioning applications, the above management methods cannot be utilized in cellular positioning in a direct way. The main reasons include two parts: 1) positioning service with PRS broadcasting is designed for UEs in a relatively large area; 2) UEs need to receive more BSs' signals than communicating with only one BS.

5G positioning enhancements in 3GPP Rel-17 aim to provide support for location latency in the order of 10 milliseconds (ms) [24]. So researchers have pointed out that future networks should also support sophisticated algorithms to design the muting configurations (MC) and operate at a different level of PRS resources to control the interference, such as a radio frame or even an orthogonal frequency division multiplexing (OFDM) symbol containing the PRS in a subframe [19], [39]. However, the design method of MC and its implementation in positioning functions have not been fully studied.

C. Main Contributions

Following the above discussion, in this paper, we design a novel muting strategy that can be efficiently managed by positioning functions in cellular networks for time-sensitive applications, where the muting configuration is generated according to an optimized set of pseudo-random sequences with considerations of concurrency and balance of PRS transmissions amongst all BSs. Furthermore, the implementation of efficient information exchange and muting coordination in positioning management functions can also be accomplished. Specifically, the main contributions of this paper are summarized as follows.

- To manage near-far interference and reduce measurement latency, a muting configuration generation method is proposed based on the combined optimization of pseudo-random sequences (CO-PRS), where the balance and concurrency of PRS transmissions among BSs are designed as selection indicators.
- The management of PRS muting in positioning functions is then analyzed in detail, in which the efficient information exchange can be achieved by transmitting the ternary seeds of pseudo-random sequences through positioning assistance data.
- For practical application purposes, we give guidance and extensive simulations on how the muting management affects the measurement latency while ensuring the required accuracy. In particular, we show the proposed CO-PRS muting can alleviate severe near-far problems in cellular networks.

The remainder of this paper is structured as follows. Section II introduces the system model, where the signal generation and time delay estimation are first derived, and the operating principle of muting management in positioning functions is then analyzed. Section III constructs the problem that minimizes the maximum UE measurement latency while ensuring the desired amount of accuracy, by optimizing the muting configurations. Section IV designs the method of muting configuration generation with the optimized set of pseudo-random sequences, which demonstrates the potential to solve the formulated problem and enable efficient information exchange. Section V presents simulation results to verify the performance of the proposed management of positioning functions. Section VI concludes the paper. Additionally, the main notations used in this paper and the corresponding physical meanings are summarized in Table I.

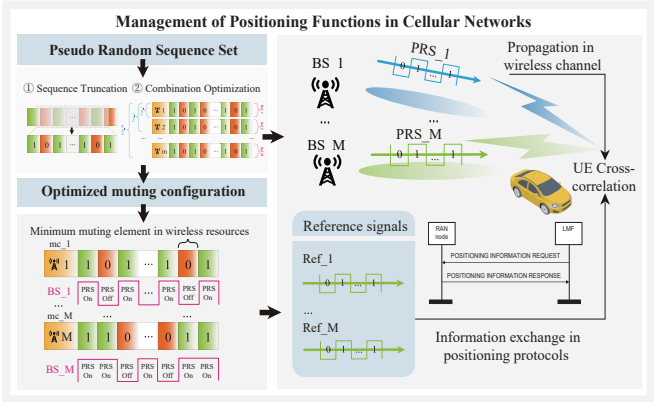

Fig. 2. Overall system model of muting management in positioning functions: (a) optimization of muting configurations and information exchange, (b) PRS transmission and time delay estimation.

II. System Model

We consider a cellular network scenario where M BSs provide communication and DL-TDOA positioning services for U UEs in the target area. As shown in Fig. 1, BS $m = \{1, \ldots, M\} \in \mathbb{M}$ are deployed in a hexagonal grid in the target area and their location has been accurately measured in advance, which is denoted by $\mathbf{b}^m = \left[\mathrm{b}_x^m, \mathrm{b}_y^m, \mathrm{b}_z^m\right]^T \in \mathbb{R}^{3\times 1}, m \in \mathbb{M}$. UE $u = \{1, \ldots, U\} \in \mathbb{U}$ located in $\mathbf{v}^u = \left[v_x^u, v_y^u, v_z^u\right]^T \in \mathbb{R}^{3\times 1}, u \in \mathbb{U}$, which are conducting time-sensitive applications and need timely location information. Positioning reference signals (PRS) transmitted by multiple BSs are superimposed at each UE receiver, which are then utilized to calculate the cross-correlation function with local reference signals to estimate the time delay or distance between the UE and target anchor BS, and finally estimate the location using multi-lateration methods. The information exchange and the coordination of multiple PRS transmission are managed by the positioning functions (also referred to location management functions (LMF)) in core networks [13], as shown in Fig. 2.

A. Signal Generation

In this subsection, the signal used for positioning purposes in cellular networks will be introduced. With the standardization process of the cellular positioning system, the dedicated positioning signal PRS has been introduced since the LTE standard [44], mapping to specific elements into the OFDM resource grid. In order to avoid undesirable interference appearing at the receiver, it is necessary to configure the muting

TABLE I
PHYSICAL MEANING OF THE MAIN NOTATIONS

Physical Meaning	Notation	Physical Meaning	Notation
Set of BS	$\mathbb{M}$	Time delay estimation with BS m	$\hat{\tau}_m$
Set of UE	$\mathbb{U}$	Error covariance of time delay estimation	Cov($\hat{\boldsymbol{\tau}}$)
Set of anchor BS of UE u	$\mathbb{M}_u$	Cumulative FIM after receiving T symbols	$\mathbf{F}_L$
Location of BS m	$\mathbf{b}^m$	Mapping function from discrete to continuous	$f(\cdot)$
Location of UE u	$\mathbf{v}^u$	Transmitted muting signal	x_m^{muting}
Length of the muting control period	L	Received muting signal	y_m^{muting}
Continuous subframes in PRS occasion	N_{PRS}	PRS symbols in each subframe	$N_{\text{symb}}^{\text{PRS}}$
Muting control sequence of BS m	mc_m	Cross-correlation function with muting	$R_{T,m}^{\mathcal{M}}$
Muting configurations of all m BS	$\mathcal{M}_m$	Required measurement accuracy	τ_{err}^{Req}
QPSK-modulated PRS sequence	$r_{l,m}$	Required received signal length	$T_{u,m}$
Pseudo-random sequence for PRS signal generation	c_{prs}	Set of pseudo-random sequences for muting control	$\mathcal{M}_{\text{prepare}}$
Complex-valued OFDM symbol	$a_{k,l,m}$	Set of generator polynomial values	$\mathcal{M}_{gp}$
OFDM baseband signal	$s_{l,m}$	Set of register values	$\mathcal{M}_{rg}$
Sampling frequency	f_s	Set of truncation points	$\mathcal{M}_{tr}$
Received signal from BS m	y_m	Temporary sequence for BS m in CO-PRS	c_m^{tr}
Cross-correlation function	$R_{T,m}$	Regeneration function for muting sequences	$g(\cdot)$

information for these BSs, which is generally controlled by a sequence mc_m composed of 0 and 1 for each BS $m \in \mathbb{M}$. Here the value 0 indicates that we mute the corresponding resource, while 1 allows normal transmission. PRS occasions have also been defined to improve positioning performance [35], including N_{PRS} continuous downlink subframes, where each subframe has $N_{\text{symb}}^{\text{PRS}}$ OFDM symbols containing the PRS. In this paper, we consider one PRS occasion as the muting control period, where the minimum unit of muting element is set as one OFDM symbol containing the PRS, as shown in the red dotted box in the OFDM resource grid in Fig. 3. Thus, the length of control sequence becomes $L = N_{\text{PRS}} N_{\text{symb}}^{\text{PRS}}$, and the muting control sequences of BS in $\mathbb{M}$ will form a set $\mathcal{M} = \{mc_1, \ldots, mc_M\}$, which will be analyzed in the Section IV. Here, the signal without muting control will be first derived, and the signal with muting control will then be introduced in Section II.C.

In the 3GPP standard [44], the quad-phase shift keyed (QPSK)-modulated PRS sequence can be expressed as

$$r_{l,n_s,m}[i] = \frac{1}{\sqrt{2}}(1 - 2c_{\text{prs}}[2i]) + j\frac{1}{\sqrt{2}}(1 - 2c_{\text{prs}}[2i+1]), \quad (1)$$

where $i = 0, 1, ..., 2N_{\text{RB}}^{\text{max,DL}} - 1$, $\forall m \in \mathbb{M}$ and n_s is the slot number within a radio frame and l is the index of the OFDM symbol within the slot. The number of the resource blocks (RB) $N_{\text{RB}}^{\text{max,DL}} = 110$ defines the largest downlink bandwidth. The pseudo-random sequence $c_{\text{prs}}[i]$ for

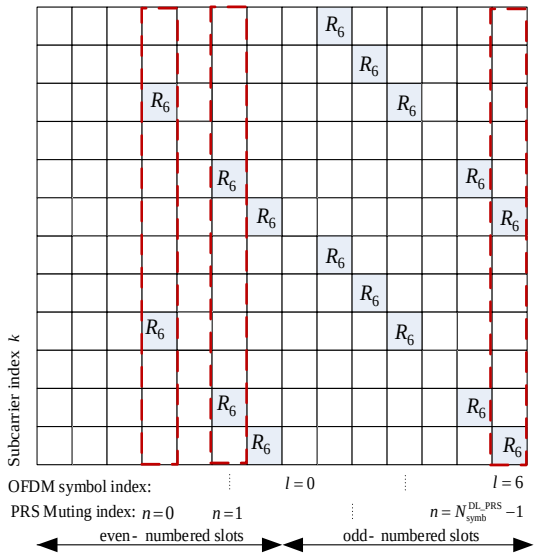

Fig. 3. PRS mapping and muting element in the OFDM resource grid, where R_6 denotes PRS symbols $a_{k,l,m}$ in antenna port 6.

PRS generation shall be initialized according to [44], in which $c_{\text{prs}}^{\text{init}} = 2^{28} \cdot \lfloor N_{\text{ID}}^{\text{PRS}}/512 \rfloor + 2^{10} \cdot (7 \cdot (n_s + 1) + l + 1) \cdot (2 \cdot (N_{\text{ID}}^{\text{PRS}} \bmod 512) + 1) + 2 \cdot (N_{\text{ID}}^{\text{PRS}} \bmod 512) + N_{\text{CP}}$, where $N_{\text{ID}}^{\text{PRS}} \in \{0, 1, ..., 4095\}$ generally equals to $N_{\text{ID}}^{\text{cell}}$. We consider normal CP with $N_{\text{CP}} = 1$ corresponds, and $N_{\text{CP}} = 0$ is for the extended CP. As shown in Fig. 3, the PRS sequence $r_{l,n_s,m}[i]$ shall then be mapped to complex-valued modulation symbols $a_{k,l,m}$ in the OFDM resource grid as reference signal for antenna port $p = 6$ in slot n_s according to

$$a_{k,l,m} = r_{l,n_s,m}[i], \quad (2)$$

where the subcarrier index k in frequency domain is generated according to

$$k = 6\left(i + N_{\text{RB}}^{\text{DL}} - N_{\text{RB}}^{\text{PRS}}\right) + (6 - l + v_{\text{shift}}) \bmod 6, \quad (3)$$

and the mapping of OFDM symbol index l in time domain is determined by

$$l = \begin{cases} 3, 5, 6 & \text{if } n_s \bmod 2 = 0, \\ 1, 2, 3, 5, 6 & \text{if } n_s \bmod 2 = 1. \end{cases} \quad (4)$$

The cell-specific frequency shift is given by $v_{\text{shift}} = N_{\text{ID}}^{\text{PRS}} \bmod 6$, which is usually determined by the cell ID as $N_{\text{ID}}^{\text{PRS}} = N_{\text{ID}}^{\text{cell}}$. In this paper, in order to study the effective muting strategy in severe interference scenarios, we consider imperfect PCID planning, where BS in $\mathbb{M}$ have the same value of $v_{\text{shift}} = N_{\text{ID}}^{\text{PRS}} \bmod 6$, and the transmitted PRS will cause relatively severe interference to the receiver. It should be noting that muting management will be conducted after the above mapping process, which will not change the original PRS sequence.

The time-continuous OFDM modulating reference signal $s_{l,m}(t)$ generation equation based on inverse fast Fourier transform (IFFT) without muting control in OFDM symbol

l can be expressed as [44]

$$s_{l,m}(t) = \sum_{k=-\left\lfloor N_{\mathrm{RB}}^{\mathrm{DL}} N_{\mathrm{sc}}^{\mathrm{RB}}/2 \right\rfloor}^{-1} a_{k^{(-)},l,m} \cdot e^{j2\pi k \Delta f t} + \sum_{k=1}^{\left\lceil N_{\mathrm{RB}}^{\mathrm{DL}} N_{\mathrm{sc}}^{\mathrm{RB}}/2 \right\rceil} a_{k^{(+)},l,m} \cdot e^{j2\pi k \Delta f t}, \tag{5}$$

for $0 \leq t < N \times T_s$, where $k^{(-)} = k + \left\lfloor N_{\mathrm{RB}}^{\mathrm{DL}} N_{\mathrm{sc}}^{\mathrm{RB}}/2 \right\rfloor$ and $k^{(+)} = k + \left\lfloor N_{\mathrm{RB}}^{\mathrm{DL}} N_{\mathrm{sc}}^{\mathrm{RB}}/2 \right\rfloor - 1$ denote negative and positive parts of the subcarriers, and $N_{\mathrm{sc}}^{\mathrm{RB}}$ denotes the number of the subcarriers in a resource block; the subcarrier spacing Δf equals to 15KHz for the PRS. The sampling frequency is f_s and the sample time $T_s = 1/f_s$, and N is the number of samples. In the following parts, we will further analyze the time delay and range estimation with respect to the transmitted PRS from each BS as derived in (5).

B. Time Delay Estimation

In this subsection, the derivation of time delay estimation and the corresponding influencing factors and their impact on the error covariance bounds will be conducted. We denote the speed of light as v_{light}, and the time delay measurement from UE u with BS m can be expressed as

$$\hat{\tau}_m = \frac{d_m}{v_{\text{light}}} + \Delta\tau_m + e_m, \tag{6}$$

where $d_m = \|\mathbf{b}^m - \mathbf{v}^u\|_2$ and $\hat{\tau}_m$ is the real 3D Euclidean distance and the corresponding time delay measurement, while the clock offset error is $\Delta\tau_m$ and the measurement error e_m is caused by noise. Here we simply denote the real time delay as $\tau_m^o = d_m/v_{\text{light}}$ for convenience, and we mainly consider the measurement error caused by near-far interference in this paper, so the synchronization error $\Delta\tau_m$ is assumed to be mitigated by some mature methods [45]. For simplicity, we consider the line-of-sight channel in an urban scenario [46], which can also be extended into a more general case in future work. The received signal $y_m(t)$ of UE from BS m can be expressed as

$$y_m(t) = h(t) * \sum\nolimits_l s_{l,m}(t) + w(t), \tag{7}$$

where $h(t)$ is the channel response function and $w(t)$ is the white Gaussian noise with power spectral density N_0. After sampling, the correlation $R(\tau)$ between received signals and local reference signals is calculated as

$$R_{T,m}(\tau) = \sum\nolimits_{n=1}^{T} y_m[n] s_m^*[n-\tau], \tag{8}$$

where T is the length of the processed received signal in the cross-correlation computation.

Before introducing the estimation method for τ, we will first analyze the performance bound of the range measurement, which is commonly represented by the Cramer-Rao lower bound (CRLB). According to [47], the estimated time delay vector $\hat{\boldsymbol{\tau}} = [\tau_1, \ldots, \tau_m, \ldots, \tau_M]^T$ using any unbiased, non-Bayesian estimator satisfies

$$\mathrm{Cov}(\hat{\boldsymbol{\tau}}) \succeq \mathbf{F}^{-1}(\boldsymbol{\tau}), \tag{9}$$

where $\mathrm{Cov}(\hat{\boldsymbol{\tau}})$ is the error covariance matrix of time delay estimation, and $\mathbf{F}(\boldsymbol{\tau})$ is the corresponding Fisher Information Matrix (FIM); the matrix inequality $\mathrm{Cov}(\hat{\boldsymbol{\tau}}) \succeq \mathbf{F}^{-1}(\boldsymbol{\tau})$ indicates that $\left(\mathrm{Cov}(\hat{\boldsymbol{\tau}}) - \mathbf{F}^{-1}(\boldsymbol{\tau})\right)$ is a positive semi-definite matrix. The FIM can be calculated by the standard formula [48]

$$\mathbf{F}(\boldsymbol{\tau}) = \left\{ -\mathbb{E}_{\mathbf{Y}(\boldsymbol{\tau})|\boldsymbol{\tau}} \left[\nabla_{\boldsymbol{\tau}} (\nabla_{\boldsymbol{\tau}} \ln \ell(\mathbf{Y}(\boldsymbol{\tau}) | \boldsymbol{\tau}))^T \right] \right\}, \tag{10}$$

where $\mathbb{E}[\cdot]$ denotes the expectation operator; $\ell(\mathbf{Y}(\boldsymbol{\tau}) | \boldsymbol{\tau})$ is the joint probability density function (PDF) of the correspond observation vector $\mathbf{Y}(\boldsymbol{\tau}) = [y_1, \ldots, y_m, \ldots, y_M]^T$ parametrized with respect to $\boldsymbol{\tau}$, and $\nabla_{\boldsymbol{\tau}}$ indicates the gradient with respect to $\boldsymbol{\tau}$. Since the FIM can be regarded as the information for parameter estimation, we denote the FIM of one OFDM symbol containing the PRS as $\mathbf{F}_{t-1,t}(\boldsymbol{\tau})$, and with the increase of the received signal length in the cross-correlation process as shown in (8), the cumulative FIM after receiving T symbols $\mathbf{F}_L(\boldsymbol{\tau})$ can be expressed as

$$\mathbf{F}_L(\tau) = \sum\nolimits_{t=1}^{T} \mathbf{F}_{t-1,t}(\tau). \tag{11}$$

As analyzed in [22], the derivation of the FIM can be utilized to calculate the variance of the time delay measurement error, which is given by

$$\sigma^2(\hat{\tau}_m) = \frac{T_{sym}^2}{8\pi^2 \cdot \sum_{t\in\mathcal{T}} SINR_m^t \cdot \sum_{k\in\mathcal{N}_c} p_k^2 \cdot k^2}, \tag{12}$$

where $T_{sym} = 1/\Delta f$ is the symbol duration of the received OFDM signal; $\mathcal{T}$ is the set of symbols containing the PRS; $\mathcal{N}_c$ is the subset of subcarriers used to transmit the PRS; p_k^2 is the relative power weight of subcarrier k; $SINR_m^t$ is the received signal-to-noise plus interference (SINR) of received signal from BS m at symbol t, which can be expressed as

$$SINR_m^t = \frac{p_m / PL_m}{\sum_{n\in\mathbb{M}_m^t, n\neq m} p_n / PL_n + p_{noise}}, \tag{13}$$

where m, n refer to the index of BS in $\mathbb{M}$; p_m the transmit power of the PRS of BS m, PL_m the path loss from BS m to UE, p_{noise} the received noise power; $\mathbb{M}_m^t$ refers to the set of BS that are not muted at symbol t and sharing the same time-frequency resources transmitting the PRS with BS m. Correspondingly, p_n is the transmission power of the PRS of BS n, and PL_n refers to the path loss from BS n to UE.

Accordingly, the CRLB of range estimation in meters can be then calculated as

$$\sigma(\hat{d}_m) = \sqrt{v_{\text{light}}^2 \sigma^2(\hat{\tau}_m)}. \tag{14}$$

As shown in Fig. 4, a typical UE with 5 surrounding BSs as anchors receives PRS from $t = 1$ to 24, and the cumulative FIM and CRLB of range estimation are shown in Fig. 4(a) and Fig. 4(b), respectively. Here, the transmission of PRS from 5 BSs is managed by 5 different random sequences with 50% duty cycle. It can be seen that the FIM constantly increase with the accumulation of received signal, which is in accordance with the derivation in (11). There are some symbols that provide nearly zero contribution to the FIM, which corresponds to the symbols that are muted by the random sequence. The FIM of anchor BS 1 increases dramatically from the first received symbol, while the FIM of other BSs increase more slowly. This is because in the simulation scenario, the UE is near to

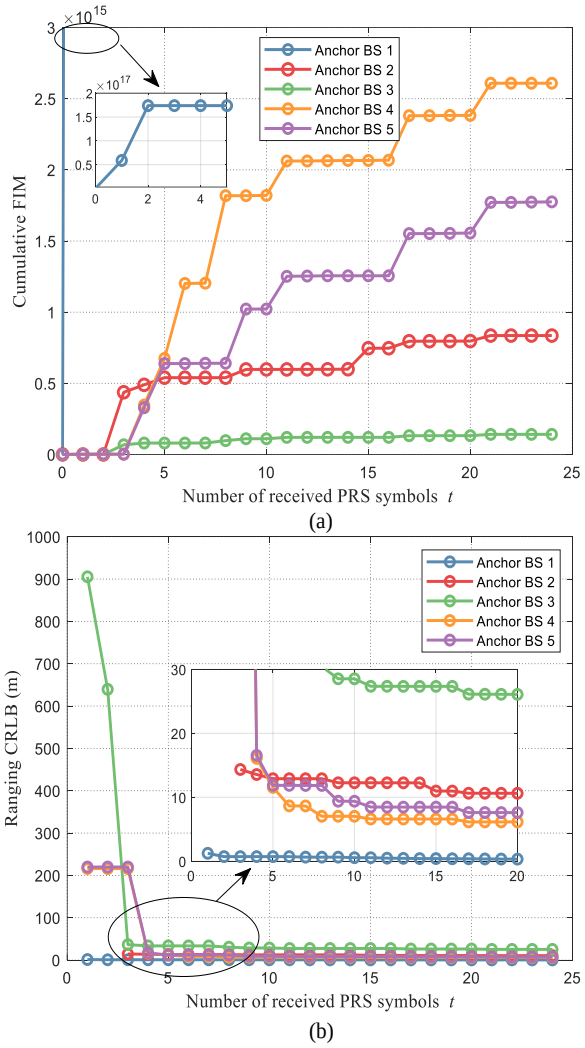

Fig. 4. An application example of cumulative (a) FIM and (b) ranging CRLB with accumulated received PRS symbols using 50% random muting functions. In this scenario, the UE is located near to anchor BS 1 and with over 250m away from anchor BS 2 to 5.

BS 1 and with over 250m away from anchor BSs 2 to 5, where the signals from BSs 2 to 5 are generally interfered with BS 1, a typical phenomenon of the near-far problems in cellular networks. Furthermore, the FIM contributed by each OFDM symbol $\mathbf{F}_{t-1,t}(\boldsymbol{\tau})$ is also different due to the received SINR as in (11)-(13), which is determined by the uncoordinated PRS transmission controlled by a random sequence. The CRLB of range estimation continuously decreases with t, and it can be seen from Fig. 4(b) that UE cannot establish a basic threshold like 10m with some anchor BSs even with a long-time cross-correlation process using $t = 24$ PRS symbols. This situation is undesirable for localization, since the WLS estimation needs at least 4 anchors to estimate the location and imbalanced ranging accuracy from BS 1 to 5 will inevitably lead to error propagation to the location update of UE [33].

Based on the above analysis and demonstration, the time delay estimation accuracy can be influenced by two main factors considered in this paper: 1) the received signal length used for cross-correlation and 2) the interference level of each received symbol. In this paper, we use the maximum likelihood estimation (MLE) to estimate the time delay between UE and each BS [20], and the first tap of the channel can be estimated according to (8) as

$$\hat{\tau}_m = \text{argmax}_\tau \left\{ R_{T,m}(\tau) \right\}, \tag{15}$$

by searching the correlation peak in the correlation function (8) to obtain the value of time delay.

Following the above guidance, the accuracy of time delay estimation can be potentially increased by utilizing a longer received signal in the measurement step and also controlling the interference level on each symbol at the same time, which can be interpreted as the correlation peak becoming higher and dominant over the noise and interference. In this case, the ML estimator can obtain the time delay with limited error τ_{err}^{Req}, i.e., $|\hat{\tau}_m - \tau_m^o| \leq \tau_{err}^{\text{Req}}$. However, for time-sensitive applications in the ITS, increasing the processed signal length to acquire accuracy improvement can also lead to certain delay to the position update of the UE, reducing the timeliness of location information. Therefore, we argue that appropriate management of multiple PRS transmission in the positioning functions have the potential to control interference and complete the position update with relatively shorter measurement latency. In the next subsection, the management of PRS transmission by muting will be derived in detail.

C. Muting Management in Positioning Functions

As analyzed in Section II.B, aiming to control the interference level and enable shorter measurement latency in cellular positioning, the positioning management functions have the responsibilities to coordinate the transmission of PRS from neighboring BS. In this paper, we focus on the muting management of PRS to achieve time-sensitive localization at the control level of each OFDM symbol, from which the normal transmission or muting of each symbol containing the PRS is determined by a binary muting control sequence $mc_m \in \mathcal{M}$ and $\forall mc_m(n) \in \{0,1\}, n \in \{1,\ldots,L\}$, as analyzed in the first part of Section II.A.

In particular, Section II.B describes a specific case where no muting management in positioning functions has been conducted, i.e., the PRS are still transmitted according to the mapping in (2) and Fig. 3, which may cause interference at the UE receiver in the scenario of a strong near-far effect among BSs, thus reducing the positioning accuracy. Although utilizing random muting control among BS can mitigate interference compared with no muting, this strategy cannot always guarantee the interference level, especially in dealing with severe near-far problems, as shown in Fig. 4. To avoid these drawbacks, PRS coordinated muting with each BS in $\mathbb{M}$ is implemented at specific OFDM symbols according to the muting configuration information $\mathcal{M}$. As shown in Fig. 2, if the PRS muting control sequence $mc_m(n) = 1$, then the reciprocal PRS symbol n of BS m will be normally transmitted, otherwise BS m will remain silent.

It should be noted that since $mc_m(n) \in \mathcal{M}$ is a discrete sequence, the muting configuration information shall be trans-

formed into time-continuous form according to the sampling rate f_s, which can be expressed as

$$mc_m(t) = f(mc_m(n)), \forall mc_m(n) \in \mathcal{M}, \tag{16}$$

where $f(\cdot)$ represents the discrete-continuous transformation function for the muting control sequence. Accordingly, the transmitted signal $x_m^{\text{muting}}(t)$ after muting control is formulated as[1]

$$x_m^{\text{muting}}(t) = mc_m(t) \times \sum\nolimits_l s_{l,m}(t), \tag{17}$$

which can be regarded as the original signal is modulated by a 0/1 sequence. Similarly, the received signal after muting control management $y_m^{\text{muting}}(t)$ of UE from BS m can be expressed as

$$y_m^{\text{muting}}(t) = h(t) * x_m^{\text{muting}}(t) + w(t). \tag{18}$$

As shown in Steps 2 and 4 in Fig. 5, according to the general cellular positioning protocols [13], the positioning functions can exchange the muting configurations in positioning assistance data[2] and let the UE generate the local reference signals x_m^{muting} corresponding to the transmitted PRS. In this way, the cross-correlation function with muting configuration $\mathcal{M}$ after sampling can be calculated as

$$R_{T,m}^{\mathcal{M}}(\tau) = \sum\nolimits_{n=1}^{T} y_m^{\text{muting}}[n]\left(x_m^{\text{muting}}\right)^*[n-\tau], \tag{19}$$

where T is the length of the processed received signal in the cross-correlation computation. Equivalently, the time delay estimation after muting management will also follow the ML method as shown in (15).

It can be seen that the accuracy of time delay estimation under muting management is mainly determined by the muting configuration $\mathcal{M}$. However, simple configurations like random muting cannot guarantee the controllable interference and may lead to a longer received signal length T for the location accuracy-timeliness trade-off. With appropriate design of $\mathcal{M}$, UE has the potential to achieve the required ranging accuracy with lower measurement latency T even under severe near-far interference. In the following sections, the problem formulation and the proposed method will be analyzed in detail.

III. Problem Formulation

In this section, the problem of reducing the latency of UE positioning in cellular networks will be summarized analytically to enable time-sensitive transportation applications. These kinds of applications typically require both accuracy and timeliness of location information, which makes it very complex to solve the original problem optimally. Therefore, in this paper, we formulate a substitute problem to acquire efficient sub-optimal solutions, by managing PRS muting configuration $\mathcal{M} = \{mc_1, \ldots, mc_M\}$ in positioning functions to reduce the measurement latency while ensuring the desired

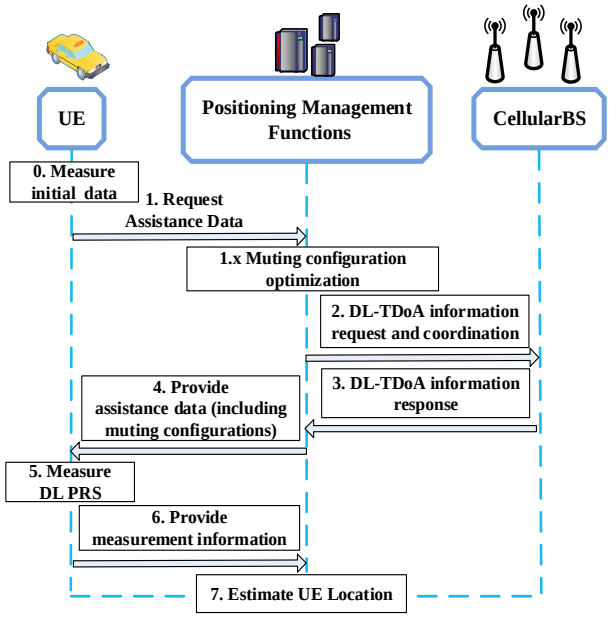

Fig. 5. Information exchange process: PRS muting managed by positioning functions in cellular networks, where the muting configurations can be transmitted through the positioning assistance data.

localization accuracy. For convenience, the evaluation metric of the measurement latency is simplified to the required received signal length T to obtain accurate ranging values in the cross-correlation process (8).

Furthermore, since the positioning performance will be significantly influenced by relative positions between UE and surrounding BS in real world, e.g., if UE u_i is located very closely to BS $m\,(\forall m \in \mathbb{M})$, while UE u_j is in a middle area of several surrounding BSs, UE u_i and u_j will experience different levels of near-far interference. Therefore, the focused problem should consider all kinds of UE's location $\mathbf{v}^u\,(\forall u \in \mathbb{U})$ in cellular networks for general performance analysis and improvement. In the design of positioning latency optimization scheme, we focus on minimizing the worst case of UE measurement latency with its anchor BS. Once these kinds of UE's performance can be guaranteed, other UEs with less severe near-far interference can also accomplish accurate localization within shorter measurement time. This formulates the substitute min-max problem. It also should be noted that the BSs in set $\mathbb{M}$ may exceed the required number of anchors for DL-TDOA positioning. Thus, the set of BSs selected as anchors by UE $u \in \mathbb{U}$ is denoted as $\mathbb{M}_u \in \mathbb{M}$, which is generated according to the BSs with strongest received signal strength (RSS) without any interference[3].

Hence, the problem of interest is formulated as

$$(\text{P1}): \min_{\mathcal{M}} \max_{u\in\mathbb{U}, m\in\mathbb{M}_u} T_{u,m} \tag{20}$$

$$\text{s.t. C1: } \hat{\tau}_{u,m} = \arg\max_{\tau} \left\{R_{T,u,m}^{\mathcal{M}}(\tau)\right\} \tag{21}$$

[1]This is equivalent to the mute the corresponding time-frequency resources in the OFMD resource grid by setting the complex symbol $a_{k,l,m} = 0$ as in (5), while the former derivation in (17) aims to demonstrate how the muting sequence control the transmitted PRS in a relatively intuitive way.

[2]Positioning assistance data may also include RAN access point position, PRS signal bandwidth and cell identity, etc., where detail information can be found in Chapter 9 of [13]. Here, we mainly focus on the muting configuration.

[3]The anchor BS selection scheme can also be selected by jointly considering the geometry and RSS between BS and UE, since the geometry dilution of precision (GDOP) can also influence the location estimation [17]. However, the BS selection is beyond the research focus of this paper and we temporarily consider a simple case.

$$\text{C2: } \left|\hat{\tau}_{u,m} - \tau^{o}_{u,m}\right| \leq \tau^{\text{Req}}_{err}, \forall u \in \mathbb{U}, m \in \mathbb{M}_u \quad (22)$$

$$\text{C3: } 1 \leq T_{u,m} \leq L+1, \forall T_{u,m} \in \mathbb{N}^{+} \quad (23)$$

where $\mathcal{M}$ is the optimization variable and the objective function is the maximum measurement latency $T_{u,m}$ of UE $u \in \mathbb{U}$ in target area with anchor BS $m \in \mathbb{M}_u$. Constraint C1 and C2 determine the objective function $T_{u,m}$ together, from which C1 represents the ML estimation process that is determined by the muting configuration $\mathcal{M}$ and the measurement latency $T_{u,m}$. Constraint C2 denotes that the estimation results $\hat{\tau}_{u,m}$ should satisfy the accuracy requirement τ^{Req}_{err} for time delay. For example, for a given optimized muting configuration $\mathcal{M}$, if $\left|\hat{\tau}_{u,m} - \tau^{o}_{u,m}\right| > \tau^{\text{Req}}_{err}$, then the accuracy constraint C2 will not be satisfied and according to C2, and the ML estimator should increase the length of processed received signal in the cross-correlation operation (8) until this constraint is met. Finally, C3 constrains the counting method of the objectives, where for the value of $T_{u,m}$, we count the number of OFDM symbols containing the PRS and then limited to a positive integer set $\mathbb{N}^{+}$. This is because the number of PRS symbols directly represents the length of the received signal, since we assume that the mapping in OFDM resource grid follows the same subframe structure as shown in Fig. 3 [44]. The maximum value of $T_{u,m}$ is set as $L+1$, which is one unit of measurement larger than the muting period $L = N_{\text{PRS}} N^{\text{PRS}}_{\text{symb}}$, meaning that UE and BS m fails to establish accurate range measurement even after processing signals with L OFDM symbols.

From another point of view, if we assume the total available resources for each BS is fixed, representing by T^{Occasion}_{m} PRS symbols in one PRS occasion, the reduction of the measurement latency $T^{\text{Occasion}}_{m} - \max_{m \in \mathbb{M}_u} T_{u,m}$ can also be regarded as the increase of resources for communication services. This is a kind of trade-off in wireless resource utilization, which is equivalent to evaluate $\max_{m \in \mathbb{M}_u} T_{u,m}$ in this paper.

IV. Proposed Method

In this section, we investigate a method to solve the above formulated problem (P1), in which we focus on the optimization of muting configuration $\mathcal{M}^{*} = \{mc^{*}_{1}, \ldots, mc^{*}_{M}\}$, so as to guarantee the worst case of UE measurement latency in cellular networks while ensuring the required amount of localization accuracy. Although the random generation of muting configurations may enable some of the UE in the middle areas between several anchor BS to meet the requirements of both delay and accuracy, this case is generally based on the premise that these UEs are less affected by near-far interference. In this case, the fairness of location services is in turn very critical for time-sensitive ITS applications, and the differing impact of interference becomes the reason why we need to consider the appropriate design of transmission control sequence, i.e., the muting configurations.

In this paper, pseudo-random sequences are utilized to generate muting configuration information, which can exhibit obvious advantages through optimized selection compared with random sequences and sequential control. The optimized pseudo-random sequence controls the interference level of each muting element, and we consider the minimum muting element is an OFDM symbol containing the PRS, as shown in Fig. 3. Note that we can also extend the minimum muting control unit to one beam of BSs, i.e., in space domain besides the time-frequency domain. In each beam, the time-frequency resource can still be muted according to the optimized $\mathcal{M}^{*}$. In this way, we can formulate a multi domain cascading management for all types of resources. The random sequence can only control an overall transmission level macroscopically, which may cause extremely high interference to the received SINR with incorrect estimation as analyzed in Section II.B. Correspondingly, random muting may also lead to very low-interference level at certain wireless resources, which is not necessary due to the gain brought by cross-correlation as in (8) and reduces the efficiency of wireless resources.

Moreover, the pseudo-random sequence is a variant of random sequence [49], which can be easily regenerated using the seed of the generator polynomial coefficients, register values and the truncation points of each sequence. These seeds can be exchanged in an efficient manner between BS, UE and the positioning management functions, rather than transmitting the whole sequences in the positioning assistance data. Especially when the muting control period L is relatively long, the transmission of the entire 0/1 sequence in $\mathcal{M}^{*}$ will increase the communication overhead significantly.

By controlling the maximum and minimum average interference concurrency in $\mathcal{M}^{*}$, we propose an algorithm for combined optimization of pseudo-random sequence (CO-PRS) through truncation and modified greedy selection, which can enable simultaneous multiple PRS transmission with controllable interference even in the case of reusing the wireless resources. The specific operation process is shown in Fig. 6 and will be derived as follows.

In this paper, we take the basic m-sequence generated by a linear feedback shift register (LFSR) [49] in the proposed CO-PRS method as an example[4], so as to illustrate the generation process for convenience. The set of pseudo-random sequences prepared for selection is denoted as $\mathcal{M}_{\text{prepare}}$, which is generated by traversing all possible generator polynomial coefficients and register values of the LFSR[5]. If we denote the order of the LFSR as d_m, the number of possible values of the polynomial and register will be 2^{dm}. Thus, each element in $\mathcal{M}_{\text{prepare}}$ follows $\forall\ c_m \in \mathcal{M}_{\text{prepare}}, c_m(n) \in \{0,1\}, n \in \{1, \ldots, L_0\}$, and its dimension is $\left(2^{dm} \times 2^{dm} \times L_0\right)$, which in order represents 1) the potential values of generator polynomial, 2) the potential values of register and 3) the length of each prepare sequence, respectively. However, due to the mismatch between the length of the prepare sequence L_0 and that of the muting period L, these sequences in $\mathcal{M}_{\text{prepare}}$ cannot be utilized as a muting control sequence in a direct way.

[4]It should be noted that the m-sequence is just one potential solution, which can also be replaced by other pseudo random sequences like the Gold sequence [44]. The auto correlation and cross-correlation characteristics of the sequences used for muting control is not a necessary requirement since the CO-PRS mainly focus on the interference management.

[5]This kind of traverse can generate a set that is beyond specific pseudo-random sequences, since each specific sequence generally limits more strict requirement on the primitive polynomial. In this paper, the properties of a specific sequence is not required, and the above process of generating $\mathcal{M}_{\text{prepare}}$ is particularly designed for the purpose of selecting muting control sequences for multiple BS.

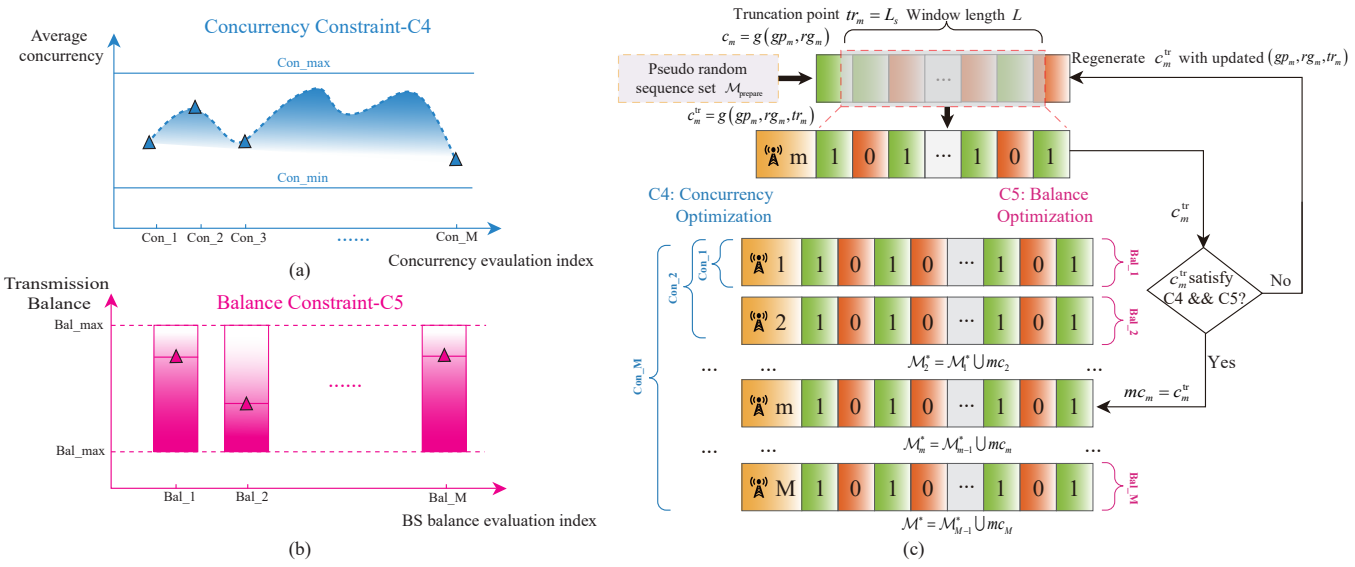

Fig. 6. Detail implementation process of the proposed CO-PRS muting configuration generation method in positioning management functions: (a) concurrency constraint, (b) balance constraint and (c) the flow diagram for the generation of $\mathcal{M}^*$.

Therefore, based on the above guidance, we should design the generation method as follows. The sequence in set $\mathcal{M}_{\text{prepare}}$ should be truncated to length L first, among which we select M elements with certain constraints, thus formulating the muting configuration information $\mathcal{M}^* = \{mc_1^*, \ldots, mc_M^*\}$. Furthermore, for each selected sequence, the corresponding generator polynomial coefficient, register value and the truncation point will be saved to form set $\mathcal{M}_{gp} = \{gp_1^*, \ldots, gp_M^*\}, \forall\ gp_i^*(n_{\text{gp}}) \in \{0,1\}, n_{\text{gp}} \in \{1, \ldots, M\}$, $\mathcal{M}_{rg} = \{rg_1^*, \ldots, rg_M^*\}, \forall\ rg_i^*(n_{\text{rg}}) \in \{0,1\}, n_{\text{rg}} \in \{1, \ldots, M\}$ and $\mathcal{M}_{tr} = \{tr_1^*, \ldots, tr_M^*\}, \forall tr_i^*(n_{\text{tr}}) \in \{0,1\}, n_{\text{tr}} \in \{1, \ldots, M\}$.

In order to control the interference level, the requirement of interference concurrency $I_{\min} \leqslant I \leqslant I_{\max}$ should be considered in the first place, which can be measured by the SINR of received signals of surrounding BS as (13) in Section II.B. However, due to the different path loss of UE $u \in \mathbb{U}$ and BS in $\mathbb{M}$ in different locations, it is difficult to evaluate the SINR quantitatively. Therefore, the requirement of interference concurrency can be transformed into the requirement of concurrency of a combined set of selected pseudo-random sequences in muting configuration $\mathcal{M}$. The temporary sequence after truncation for BS m is denoted as c_m^{tr}, and the concurrency metric is defined as

$$\text{Con}\left(c_m^{\text{tr}}\right) \triangleq 100\% \times \sum_{n=1}^{L} \left(\left(\sum_{i=1}^{m} c_m^{\text{tr}}(n) \right) / m \right) / L \quad (24)$$

where $2 \leq m \leq M$. In particular, the concurrency limit can also be set in each muting control element, which can be expressed as $\text{Con}\left(c_m^{\text{tr}}(n)\right) \triangleq 100\% \times \left(\sum_{i=1}^{m} c_i(n)\right)/m$. However, this requirement is relatively too strict and may lead to difficulties when setting the threshold, e.g., if the concurrency requirement on a single muting element is not satisfied, the iteration should be restarted and will greatly prolong the search time.

Moreover, in order to ensure the hearability of each BS and the efficient utilization of both wireless and hardware resources, the minimum and maximum transmission ratio of each BS in a muting control period should also balanced amongst BSs, which can be expressed as

$$\text{Bal}\left(c_m^{\text{tr}}\right) \triangleq 100\% \times \left(\sum_{n=1}^{L} c_m^{\text{tr}}(n) \right) / (L). \quad (25)$$

The above two constraints designed for the generation of $\mathcal{M}$ can be added to the previous problem P1 in Section III (20) and thus formulate (P2), which can be expressed as

$$(\text{P2}): \min_{\mathcal{M}} \max_{u \in \mathbb{U}, m \in \mathbb{M}_u} T_{u,m} \quad (26)$$

$$\text{s.t. } (21), (22), (23) \quad (27)$$

$$\text{C4: } \text{Con}_{\min} \leqslant \text{Con}\left(c_m^{\text{tr}}\right) \leqslant \text{Con}_{\max}, \forall c_m^{\text{tr}} \in \mathcal{M} \quad (28)$$

$$\text{C5: } \text{Bal}_{\min} \leqslant \text{Bal}\left(c_m^{\text{tr}}\right) \leqslant \text{Bal}_{\max}, \forall c_m^{\text{tr}} \in \mathcal{M} \quad (29)$$

where $\text{Con}_{\min}$, $\text{Bal}_{\min}$ and $\text{Bal}_{\min}$, $\text{Bal}_{\min}$ denote the minimum and maximum threshold on concurrency and balance of the muting control sequences in $\mathbb{M}$, respectively. Accordingly, the intuitive demonstration of constraints C4 and C5 are shown in Fig. 6(a) and Fig. 6(b). It is noteworthy that constraints C4 and C5 are not completely coincident, but complementary.

Algorithm 1 shows the muting configuration generation algorithm based on combined optimization of pseudo-random sequences (CO-PRS), and the corresponding flow diagram is shown in Fig. 6(c). The detail explanation of the CO-PRS is as follows. During the selection process for the m-th BS, the positioning management function first selects a random pseudo-random sequence c_m that has not been used from the prepare set $\mathcal{M}_{\text{prepare}}$, and then a random truncation start point L_s is selected, which needs to ensure that the truncation will not exceed the final bit of c_m. Then, c_m will be truncated from L_s with length of the muting control period L and form a temporary sequence c_m^{tr}. For the first BS, only the transmission balance $\text{Bal}\left(c_1^{\text{tr}}\right)$ will be checked, as shown in steps 12-14 in Algorithm 1, while for other BSs, the concurrency $\text{Con}\left(c_m^{\text{tr}}\right)$

Algorithm 1 Muting Configuration Generation in Positioning Functions based on Combined Optimization of Pseudo-random Sequences (CO-PRS)

Input: $\mathcal{M}_{\text{prepare}} \in \mathbb{Z}^{\left(2^{dm}\times 2^{dm}\times L_0\right)}$, $\text{Con}_{\min}$, $\text{Con}_{\max}$, $\text{Bal}_{\min}$, and $\text{Bal}_{\max}$.

Output: $\mathcal{M}^* = \{mc_1^*, \ldots, mc_M^*\}, \mathcal{M}^*{}_{gp} = \{gp_1^*, \ldots, gp_M^*\}, \mathcal{M}^*{}_{rg} = \{rg_1^*, \ldots, rg_M^*\}$ and $\mathcal{M}^*{}_{tr} = \{tr_1^*, \ldots, tr_M^*\}$.

1: **for** $m \leftarrow 1$ **to** M **do**
2: $judge \leftarrow 1$;
3: **while** $judge$ **do**
4: Select a pseudo-random sequence c_m randomly from initial set $\mathcal{M}_{\text{prepare}}$;
5: $gp_m \leftarrow$ polynomial coefficients of c_m;
6: $rg_m \leftarrow$ initial values of register of c_m;
7: Judge whether c_m has been used, and if so, choose again;
8: $L_s \leftarrow rand\,(1, L_0 - L + 1)$;
9: $judge\_tmp \leftarrow 1$;
10: **while** $judge\_tmp$ & $Ls \leq (L_0 - L + 1)$ **do**
11: The sliding window of length L takes L_s as the left end point, and truncates c_m to get c_m^{tr};
12: **if** $m == 1$ **then**
13: Calculate $\text{Bal}\,(c_m^{\text{tr}})$ using (25);
14: **if** $\text{Bal}_{\min} \leq \text{Bal}\,(c_m^{\text{tr}}) < \text{Bal}_{\max}$ **then**
15: $mc_1^* \leftarrow c_m^{\text{tr}}$, $judge\_tmp \leftarrow 0$, $judge \leftarrow 0$, $gp_1^* \leftarrow gp_m$, $rg_1^* \leftarrow rg_m$ and $tr_1^* \leftarrow Ls$;
16: **else**
17: $L_s \leftarrow L_s + 1$;
18: **end if**
19: **else**
20: Calculate $\text{Con}\,(c_m^{\text{tr}})$ and $\text{Bal}\,(c_m^{\text{tr}})$ using (24) and (25);
21: **if** $\text{Con}_{\min} \leq \text{Con}\,(c_m^{\text{tr}}) \leq \text{Con}_{\max}$ & $\text{Bal}_{\min} \leq \text{Bal}\,(c_m^{\text{tr}}) < \text{Bal}_{\max}$ **then**
22: $mc_m^* \leftarrow c_m^{\text{tr}}$, $judge\_tmp \leftarrow 0$, $judge \leftarrow 0$, $gp_m^* \leftarrow gp_m$, $rg_m^* \leftarrow rg_m$ and $tr_m^* \leftarrow Ls$;
23: **else**
24: $L_s \leftarrow L_s + 1$;
25: **end if**
26: **end if**
27: **end while**
28: **end while**
29: **end for**

and $\text{Bal}\,(c_m^{\text{tr}})$ will both be checked. If c_m^{tr} satisfies the above requirements, the positioning functions will let c_m^{tr} be the muting control sequence for BS m, corresponding to steps 20-22. Otherwise, the positioning functions will regenerate a temporary sequence by moving the truncation start point, as shown in steps 17 and 24. In particular, if the change of truncation still does not match the requirement in (P2), as steps 4-6 in Algorithm 1 will show, the positioning functions will repeat the selection in the prepare set to find a new sequence c_m. In summary, the selection process for BS m can be expressed as

$$mc_m = \begin{cases} c_m^{\text{tr}}, \text{ if } \text{Bal}_{\min} \leqslant \text{Bal}\left(c_m^{\text{tr}}\right) \leqslant \text{Bal}_{\max} \\ \text{ and } \text{Con}_{\min} \leqslant \text{Con}\left(c_m^{\text{tr}}\right) \leqslant \text{Con}_{\max}; \\ \text{regenerate } c_m^{\text{tr}}, \text{ otherwise.} \end{cases} \tag{30}$$

Thereafter, in a greedy manner, the muting control sequence of the next BS will be configured by repeating the above steps until the last one is reached. The optimized set of muting configurations at iteration m is denoted as $\mathcal{M}_m^*$, which is formulated according to

$$\mathcal{M}_m^* = \mathcal{M}_{m-1}^* \cup mc_m \tag{31}$$

where $2 \leqslant m \leqslant M$. After the muting configuration $\mathcal{M}^* = \mathcal{M}_M^*$ is configured, Algorithm 1 will output $\mathcal{M}^*$ and its corresponding set of generator polynomial coefficients $\mathcal{M}^*{}_{gp}$, register values $\mathcal{M}^*{}_{rg}$ and truncation points $\mathcal{M}^*{}_{tr}$.

The management of positioning functions will be introduced together with Fig. 5 from Section II.B as follows. First, the proposed CO-PRS process will be implemented in step 1.x as shown in Fig. 5, and in step 2 and 3, the positioning functions coordinates BS in $\mathbb{M}$ to transmit the PRS by the pre-configured muting information $\mathcal{M}^*$. In particular, to achieve efficient management of positioning services, the positioning management function shall only exchange the "ternary seeds" (gp_m, rg_m, tr_m) in the positioning assistance data [19]. This will be utilized to regenerate the entire muting control sequences instead of transmitting $\mathcal{M}^*$, as shown in step 4 in Fig. 5, which can be expressed as

$$mc_m = g\,(gp_m, rg_m, tr_m) \tag{32}$$

where $g\,(\cdot)$ represents the regeneration function. For example, if the prepare set $\mathcal{M}_{\text{prepare}}$ is known in both BSs and UEs sides through the positioning functions, both of them can regenerate mc_m using (gp_m, rg_m, tr_m) as indices in the 3-dimensional matrix formulated by $\mathcal{M}_{\text{prepare}}$. In step 5, the UE needs to calculate the cross-correlation function with the local reference signal of anchor BS in $\mathbb{M}_u$, which can be regenerated by function $g\,(\cdot)$ and the seeds exchanged from step 4. Finally, the UE measurement results will be returned to the positioning functions to estimate the location of UE, which corresponds to the steps 6-7 in Fig. 5.

V. Simulation Results and Discussion

In this section, a series of numerical simulations are conducted to evaluate the performance of the proposed muting management in positioning functions.

The main parameters are listed as follows. As shown in Fig. 8, we consider a cellular network scenario with $M = 19$ BS deployed in a hexagonal grid with inter site distance (ISD) of 300m, which is a common assumption for cellular positioning simulations [35]. The height of BS in meters follows the distribution of $\text{b}_z^m \sim \mathcal{N}\left(15, 2^2\right), \forall m \in \mathbb{M}$, and the height of UE is set as 1.5m. The muting control period is set as $N_{\text{PRS}} = 3$ consecutive subframes in a PRS occasion, where each subframe contains $N_{\text{symb}}^{\text{PRS}} = 8$ symbols with PRS following the mapping in Fig. 3, and the muting control period in unit of PRS symbol, i.e., the sequence truncation length is obtained

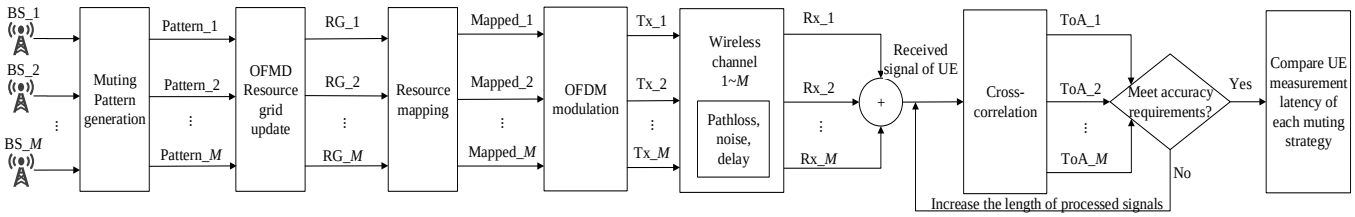

Fig. 7. Simulation process to evaluate the measurement latency of different muting management method in positioning functions.

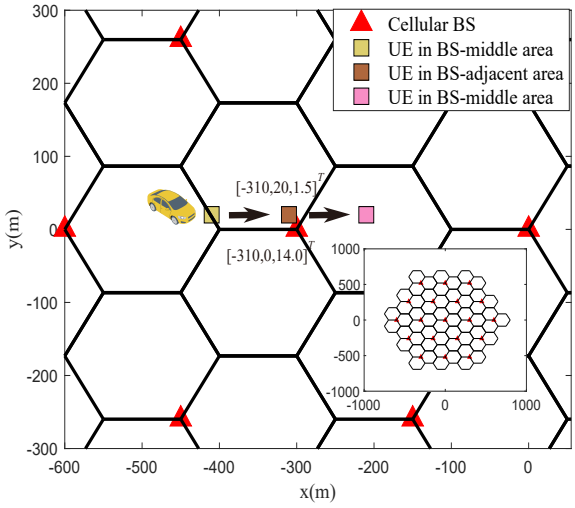

Fig. 8. Simulation scenario: 19 cellular BS deployed in a hexagonal grid with inter site distance of 300 m, and UE are moving from a BS-middle to BS-adjacent and finally stop to BS-middle area.

as $L = N_{\text{PRS}} N_{\text{symb}}^{\text{PRS}} = 24$. The central frequency is 3.5GHz, and the subcarrier spacing is 15kHz. The bandwidth allocation of the proposed system is set as $N_{\text{RB}}^{\text{DL}} = N_{\text{RB}}^{\text{PRS}} = 100$, which equals to $B = 20$MHz, and the sampling frequency is set as $f_s = 122.88$MHz for the considerations of analyzing the system performance with finer resolution. In particular, the values of the PRS frequency shift of each BS are assumed as the same since we mainly focus on the extreme situation where strong near-far interference exists, i.e., $v_{\text{shift}} = N_{\text{ID}}^{\text{PRS}} \bmod 6$ and the cell ID $N_{\text{ID}}^{\text{cell}} = 0, 6, 12, \ldots, 108$ with $N_{\text{ID}}^{\text{PRS}} = N_{\text{ID}}^{\text{cell}}$. The transmit power of each BS is 36dBm. The noise power of the additive white Gaussian noise in wireless channel is $N_0 B$, where the noise power per Hertz $N_0 = -174$dBm/Hz following the Boltzmann formula. The number of anchor BSs in each $\mathbb{M}_u$ is $N_{\text{anchor}} = 5$, and the accuracy requirement is set as $\tau_{err}^{\text{Req}} = 10$m. The MC of BSs are generated according to the proposed CO-PRS method. For the generation of the prepare set, the order of the LFSR is set as $dm = 9$, and the number of possible generator polynomial coefficients and register values both equal to $2^{dm} = 2^9 = 512$. The constraint threshold values $\text{Bal}_{\max} = 36\%$, $\text{Bal}_{\min} = 10\%$, $\text{Con}_{\min} = 30\%$, $\text{Con}_{\max} = 40\%$.

The simulation results are obtained through the flow diagram as shown in Fig. 7. First, the muting configurations are generated according to different muting management methods. Here, besides the proposed CO-PRS muting, we mainly consider benchmark methods, which include 4 random muting strategies with different levels of duty cycles ranging from 10% to 70% and also the ideal muting with sequential PRS transmission. After the generation of muting configurations, each BS can map the original data to the OFDM resource grids after muting control for OFDM modulation according to Section II.A and C. The transmission signals are then transformed into the received signal with simulated urban line-of-sight channel model in [46], in which the path loss, noise and time delay are all considered, and the BSs and UEs are equipped with omni-directional antenna for convenience. The received signal superimposed with multiple PRS at the UE receiver u will be cross-correlated with the local reference signal, which has been exchanged with the positioning management function as analyzed in Section II.B. The ML estimator will estimate the time delay and in the simulation part we will compare the time delay estimation with the ground truth that has been added in the simulated wireless channel. If the accuracy requirement of τ_{err}^{Req} has not been achieved with all of its anchor BSs in $\mathbb{M}_u$, one more PRS symbol will be added in the received signal to update $R_{T,m}^{\mathcal{M}}$ with $T = T+1$ for more accurate estimation; and when the requirement is satisfied, the corresponding length of processed signals in unit of PRS symbols will be recorded as the measurement latency $\max(T_{u,m})$.

In typical transportation applications, moving vehicles usually traveling along an urban street, where the distance between this moving UE and a far-away BS may first experience over a couple of hundred meters and with the movement reducing to tens of meters, and finally leaves behind this BS, increasing the BS-UE distance again. In this process, the interference brought by this BS is generally from weak to strong and then to weak, which may lead to a significant impact on both the accuracy and timeliness of cellular positioning. Therefore, in order to provide guidance for practical ITS applications and analyze the general performance of the proposed muting management in cellular networks, shown in Fig. 8, we tested various position relationship between moving vehicle UE and BS, where the UE moves linearly from $(-410, 20)^T$, which is far from surrounding BS, to $(-310, 20)^T$ that is very close to the BS deployed at $(-300, 0)^T$ and finally stop at $(-210, 20)^T$. Intervals between $(-410, -330)^T$ and $(-270, -210)^T$ are referred to below as the "BS-middle area", and the interval $(-330, -310)^T$ is regarded as the "BS-

[7]The solid dot in each PRS correlation function represents the correlation peak, which may not be the position corresponding to the true time delay since random noise and interference is also present.

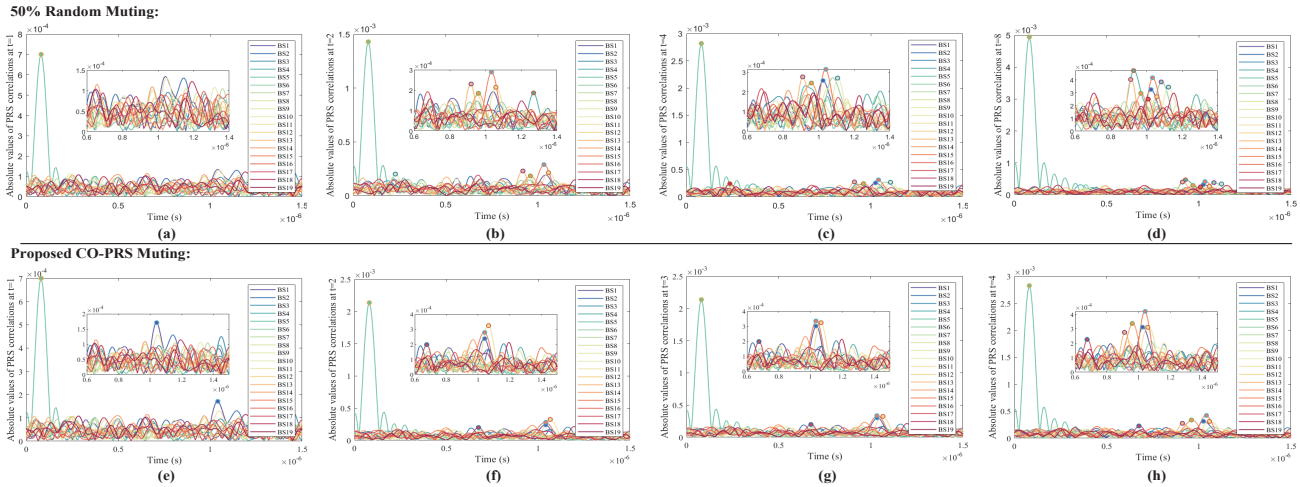

Fig. 9. Two application examples of PRS correlations before achieving the required accuracy using 50% random benchmark and the proposed CO-PRS muting management, where the UE is located in $(-310, 20)^T$ from $t = 1$ to $t = T_{u,m}$[7]: from (a) to (d), the number of qualified anchor (i.e., the accuracy of UE measurement with its anchor BS has achieved the requirement τ_{err}^{Req}) with 50% random muting from $t = 1$ to $t = 8$ are 1, 3, 4, 3, 2, 3, 4, 5, respectively, which needs $T_{u,m} = 8$ symbols to complete accurate measurement, while from (e) to (h) with the CO-PRS only needs $T_{u,m} = 4$ symbols to achieve the same requirement.

adjacent area". Since the BS deployment presents a standard hexagonal grid with symmetry, the positioning performance of UE on this trajectory can approximately represent the positioning performance of UE in $\mathbb{U}$ in the target area of a typical cellular scenario.

Here we analyze the positioning performance of UE located in the BS-adjacent area first, whose coordinates is $(-310, 20)^T$, and then statistical simulations will be carried out. Fig. 9 shows two application examples of PRS correlations $R_{T,m}^{\mathcal{M}}$ at different T before achieving the required accuracy using the 50% random benchmark and the proposed CO-PRS muting management. Fig. 9(a) to Fig. 9(d) corresponds to the 50% random muting management, where the number of anchors that satisfy $\left|\hat{\tau}_{u,m} - \tau_{u,m}^{o}\right| \leq \tau_{err}^{\text{Req}}, \forall m \in \mathbb{M}_u$, i.e., the qualified anchors, increases slowly from 1 to $N_{\text{anchor}} = 5$, requiring 8 symbols to complete the position update with the required amount of accuracy ($\max(T_{u,m}) = 8$). For comparison, the PRS correlations $R_{T,m}^{\mathcal{M}^*}$ with the proposed CO-PRS muting management are shown from Fig. 9(e) to Fig. 9(h), in which the number of qualified anchors increases quickly from 1 to 5 using only 4 symbols, i.e., $\max(T_{u,m}) = 4$, reducing the measurement latency by about 50%.

It should be noted that Fig. 9 only shows the positioning performance from one-time realization as an example for the UE situated in $(-310, 20)^T$. To make the results more statistically significant, through Monte-Carlo simulations repeated 128 times, we analyze the CDF of UE measurement latency in BS-adjacent area as shown in Fig. 10. Here we take the ratio of UE who have completed the position update within certain signal length t as the evaluation metric for convenience, and the corresponding result of the proposed optimized method is denoted as p_o and the random benchmark as p_{b_i} ($i = 10, 30, 50$ and 70 for comparison), representing the random muting with different value of duty cycle. It can be seen from Fig. 10 that for the proposed optimized CO-PRS muting, the measurement latency is much lower than that of

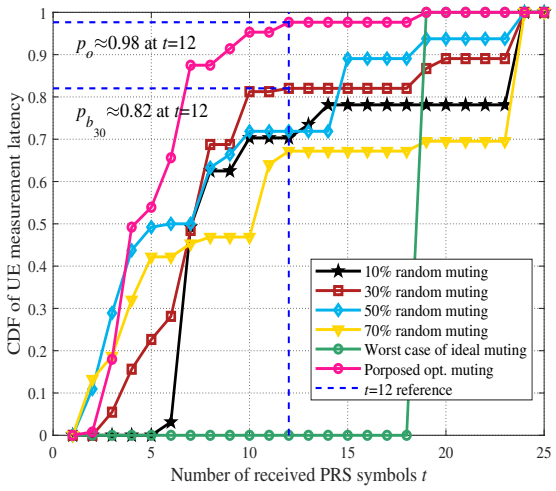

Fig. 10. Statistical results of UE measurement latency for UE located in $(-310, 20)^T$, which is in the referred BS-adjacent area.

the random benchmarks. For example, when $t = 12$, p_o is approximately equal to 0.98, meaning that almost 98% of UEs are able to achieve the required accuracy within half of the muting control period, while $p_{b_{30}}$ is roughly equal to 0.82. In particular, when the worst case of the ideal muting benchmark method is considered, BSs in $\mathbb{M}$ transmit signal in turn on each symbol, and the UE has to wait for position update until the last BSs in $\mathbb{M}_u$ finishes the transmission, which may lead to severe latency for this case. As shown in the right part of Fig. 10, the green line remains at 0 for the first 18 PRS symbols and rises to 1 steeply at the 19-th PRS symbol. For a single UE, the best result of ideal muting will be proportional to the number of BSs required for positioning, i.e., $\max_{m \in \mathbb{M}_u} T_{u,m} \propto N_{\text{anchor}}$. However, for more practical use cases including multiple UEs with a large amount of BSs

$M \geqslant N_{\text{anchor}}$, the optimal muting order of the ideal muting is difficult to determine and the best measurement latency of UEs in each places will be different. Therefore, we only show the worst case of ideal muting in Fig. 10 for simplicity. Since the time-sensitive transportation applications require the position information with high timeliness, such measurement latency in positioning service is undesirable. The proposed CO-PRS muting only takes 2.28ms corresponding to $t = 12$ to make 98% of the UEs satisfy the accuracy requirement, while other muting strategies like 50% random muting will require at least 3.64ms. This reveals that the measurement latency has been effectively reduced by about 37% and is thus essential for improving the timeliness of the location information.

It is noteworthy that results in Fig. 9 and Fig. 10 focus on the UE in BS-adjacent areas, which is only one kind of situation in a typical trajectory of transportation applications. However, in other points on the trajectory in Fig. 8, the impact of near-far problems on UE positioning may be different. The performance improvement of the proposed CO-PRS relative to the random benchmarks when the UE is located in different areas is tested, which is shown in Fig. 11. The performance metric of the improvement between the proposed method and benchmarks is calculated by averaging the ratios of p_o/p_{b_i} through Monte-Carlo simulations. According to the problem (P1) formulated in Section III, a larger value of p_o/p_{b_i} is preferred in this research. With intervals of $20m$ from $(-410, 20)^T$ to $(-210, 20)^T$, the improvement of p_o relative to each p_{b_i} is shown using histograms with the color corresponds to each benchmark method, and the average performance improvement is shown as the solid pink line in Fig. 11.

It can be seen that when the UE is located in the BS-middle area, which is approximately from $(-410, 20)^T$ to $(-330, 20)^T$ and also $(-270, 20)^T$ to $(-210, 20)^T$, the ratios of p_o/p_{b_i} are nearly equal to 1 because the interference caused by surrounding BS is generally tolerable, which leads to a relatively lower measurement latency of the UE for all muting management methods. In BS-middle area, the management in positioning functions seems unnecessary. However, the near-far interference will be extremely high when the UE is in the BS-adjacent area, which is around locations from $(-310, 20)^T$ to $(-290, 20)^T$. This is possibly because the relatively higher received signal power of BS deployed at $(-300, 0)^T$ makes the signals from other neighboring BS nearly unrecognizable. This effect will then be analyzed quantitatively in Fig. 12. In BS-adjacent area, the average ratios of p_o/p_b are typically higher, ranging from 1.18 to 1.43. The effectiveness of the proposed method has been highlighted in this scenario, since the proposed CO-PRS muting is able to control the concurrency to an acceptable level and limit the transmission balance among BSs at the same time.

Fig. 12 shows the harmonic average SINR[8] (which is referred to below as the SINR for simplicity) of the received signals along the same trajectory in Fig. 8 and Fig. 11. In both BS-middle and BS-adjacent area, the SINR of the CO-

[8]In this paper, the harmonic average is selected since it can better reflect the impact of weaker ones, and the SINR of the nearest two BS are also not considered since their signals are usually too strong and UE is able to complete measurement of them in a relatively short time.

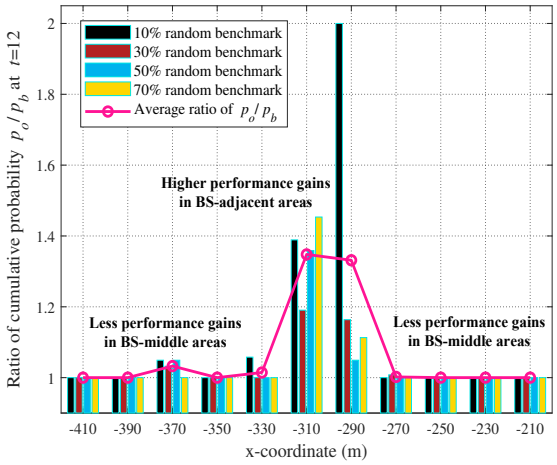

Fig. 11. Statistical results of a moving UE from a BS-middle to BS-adjacent and finally stop at a BS-middle area: the improvement ratio brought by the proposed CO-PRS positioning functions, i.e., the value of p_o/p_{b_i} ($i = 10, 30, 50$ and 70 for benchmark comparison).

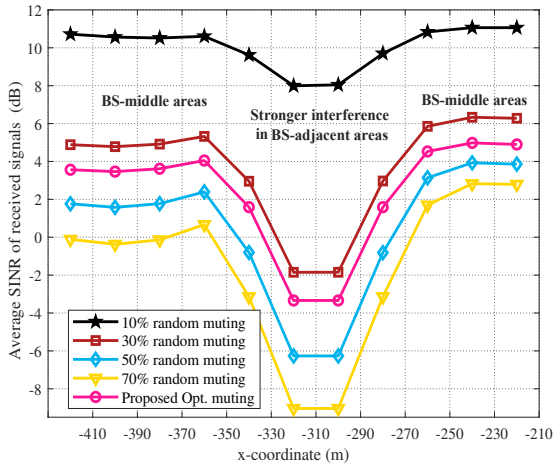

Fig. 12. Statistical results corresponding to the same UE trajectory of Fig. 8: the average SINR of the received PRS from BS except the nearest two achieved by different muting management.

PRS is relatively higher compared with 50% and 70% random muting strategies, and lower than that of the 10% and 30% random benchmarks. While in the BS-middle area, the near-far interference value is relatively lower, which is tolerable for accurate measurement, and the UE is able to complete measurement with in a short time, as shown in the left and right part of Fig. 11. Correspondingly, in the BS-adjacent area, the SINR descends rapidly in the middle of Fig. 12, which is in accordance with the trends in the middle of Fig. 11. This phenomenon supports the reason why the proposed CO-PRS can achieve better performance in the BS-adjacent area, where the proposed method can control the balance and concurrency for multiple PRS transmission. However, the 10% and 30% random muting cannot ensure the hearability of BS, and the muting benchmarks with higher duty cycles cannot ensure the concurrency of interference. This means

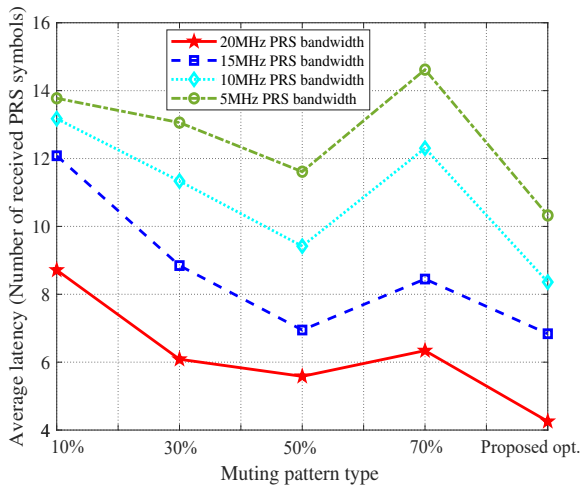

Fig. 13. Average measurement latency of each muting methods realized by different PRS bandwidth.

they both yield undesirable latency results compared with the CO-PRS method. Range-based localization estimation requires measurements with more than 4 anchor BSs, and a lower transmission ratio without balance control may become insufficient for WLS estimation. In summary, the proposed muting management method can significantly reduce the measurement latency while maintaining accurate localization, especially when dealing with severe near-far problems.

Since the setting of the PRS bandwidth will also influence the positioning performance in practical applications, the impacts of the PRS bandwidth under different muting strategies are also analyzed. It can be seen from Fig. 13 that the measurement latency decreases with the increase of PRS bandwidth under each muting method, and the proposed CO-PRS still performs the best among the benchmarks. A larger PRS bandwidth in the frequency domain will reduce the estimation error, from which the UE can meet the positioning accuracy requirements with less resources in the time domain. When the PRS bandwidth is 5MHz, there is a 30% improvement over the maximum delay, which reflects that the proposed CO-PRS method has great potential in saving bandwidth, and the remaining bandwidth can be utilized for communication purposes. In summary, the proposed CO-PRS muting management method can effectively reduce the latency for many wireless resource allocation situations.

VI. Conclusion

In this paper, we focus on the management of positioning functions in cellular networks, aiming to enable both accurate and high timeliness localization service for time-sensitive transportation applications. To reduce the measurement latency caused by the common near-far interference, a muting configuration generation method is proposed based on combined optimization of pseudo-random sequences (CO-PRS) with balance and concurrency considerations. The management of muting in positioning functions has also been analyzed, where the efficient information exchange can be achieved by the ternary seeds used for regenerating the control sequences in assistance data under existing positioning protocols. Simulation results verify that the proposed CO-PRS muting managed by positioning functions can effectively reduce the measurement latency while ensuring the required localization accuracy even in the scenario of severe near-far problems. The average improvement ratio ranges from 18% to 43% compared with the conventional random and ideal muting benchmarks.

Therefore, we foresee that network management of positioning functions has the potential to play a vital role in the future cellular networks, especially for the ITS applications. Future work is in progress to consider 1) muting management based on beamforming design with MIMO, and 2) cooperative information exchange managed by positioning functions to achieve quick and accurate positioning in V2X systems.

References

[1] H. Huang, G. Gartner, J. M. Krisp, M. Raubal, and N. Weghe, "Location based services: ongoing evolution and research agenda," *Journal of location based services*, 2018.

[2] A. Ullah, X. Yao, S. Shaheen, and H. Ning, "Advances in position based routing towards ITS enabled fog-oriented VANET–a survey," *IEEE Transactions on Intelligent Transportation Systems*, vol. 21, no. 2, pp. 828–840, 2020.

[3] A. Eskandarian, C. Wu, and C. Sun, "Research advances and challenges of autonomous and connected ground vehicles," *IEEE Transactions on Intelligent Transportation Systems*, vol. 22, no. 2, pp. 683–711, 2021.

[4] C. Cao, Z. Li, P. Zhou, and M. Li, "Amateur: Augmented reality based vehicle navigation system," in *Proceedings of the ACM on Interactive, Mobile, Wearable and Ubiquitous Technologies (UbiComp '19)*, vol. 2, no. 4, pp. 1–24, 2018.

[5] P. Ghorai, A. Eskandarian, Y.-K. Kim, and G. Mehr, "State estimation and motion prediction of vehicles and vulnerable road users for cooperative autonomous driving: A survey," *IEEE Transactions on Intelligent Transportation Systems*, vol. 23, no. 10, pp. 16 983–17 002, 2022.

[6] C.-Y. Chen and W.-R. Wu, "Three-dimensional positioning for LTE systems," *IEEE Transactions on Vehicular Technology*, vol. 66, no. 4, pp. 3220–3234, 2017.

[7] Z. Wang, R. Liu, Q. Liu, L. Han, J. S. Thompson, Y. Lin, and W. Mu, "Toward reliable uav-enabled positioning in mountainous environments: System design and preliminary results," *IEEE Transactions on Reliability*, vol. 71, no. 4, pp. 1435–1463, 2022.

[8] S. Stephenson, X. Meng, T. Moore, A. Baxendale, and T. Edwards, "Implementation of V2X with the integration of network RTK: Challenges and solutions," in *25th International Technical Meeting of the Satellite Division of the Institute of Navigation (ION GNSS 2012)*, Nashville, TN, 2012, pp. 1556-1567.

[9] Z. Wang, R. Liu, Q. Liu, L. Han, and W. Mu, "Controllable positioning service with uav-enabled cooperative jamming," *IEEE Wireless Communications Letters*, vol. 10, no. 9, pp. 1929–1933, 2021.

[10] 3GPP TS 36.305, "Stage 2 functional specification of user equipment (UE) positioning in E-UTRAN," Std., Rel. 13, Dec. 2015.

[11] S. Chen, J. Hu, Y. Shi, L. Zhao, and W. Li, "A vision of C-V2X: Technologies, field testing, and challenges with chinese development," *IEEE Internet of Things Journal*, vol. 7, no. 5, pp. 3872–3881, 2020.

[12] J. A. del Peral-Rosado, R. Raulefs, J. A. López-Salcedo, and G. Seco-Granados, "Survey of cellular mobile radio localization methods: From 1G to 5G," *IEEE Communications Surveys Tutorials*, vol. 20, no. 2, pp. 1124–1148, 2018.

[13] 3GPP TS 38.455, "NG-RAN; NR Positioning Protocol A (NRPPa)," Std., Rel. 16, July. 2021.

[14] C. Pan, M. Elkashlan, J. Wang, J. Yuan, and L. Hanzo, "User-centric C-RAN architecture for ultra-dense 5G networks: Challenges and methodologies," *IEEE Communications Magazine*, vol. 56, no. 6, pp. 14–20, 2018.

[15] N. Bhushan, J. Li, D. Malladi, R. Gilmore, D. Brenner, A. Damnjanovic, R. T. Sukhavasi, C. Patel, and S. Geirhofer, "Network densification: The dominant theme for wireless evolution into 5G," *IEEE Communications Magazine*, vol. 52, no. 2, pp. 82–89, 2014.

[16] R. Zhang, F. Yan, W. Xia, S. Xing, Y. Wu, and L. Shen, "An optimal roadside unit placement method for VANET localization," in *2017 IEEE Global Communications Conference (GLOBECOM)*, 2017, pp. 1–6.

[17] Q. Liu, R. Liu, Z. Wang, L. Han, and J. S. Thompson, "A V2X-integrated positioning methodology in ultradense networks," *IEEE Internet of Things Journal*, vol. 8, no. 23, pp. 17 014–17 028, 2021.

[18] H. Zhang, M. Feng, K. Long, G. K. Karagiannidis, and A. Nallanathan, "Artificial intelligence-based resource allocation in ultradense networks: Applying event-triggered Q-learning algorithms," *IEEE Vehicular Technology Magazine*, vol. 14, no. 4, pp. 56–63, 2019.

[19] A. Mirbagheri and B. C. Banister, "Randomization of PRS frequency offsets and muting patterns in LTE for EOTDOA," U.S. Patent 10 439 775B2, Sep. 1, 2015.

[20] H. Rydén, S. M. Razavi, F. Gunnarsson, S. M. Kim, M. Wang, Y. Blankenship, A. Grövlen, and A. Busin, "Baseline performance of LTE positioning in 3GPP 3D MIMO indoor user scenarios," in *2015 International Conference on Localization and GNSS (ICL-GNSS)*, 2015, pp. 1–6.

[21] Q. Liu, R. Liu, Z. Wang, and Y. Zhang, "Simulation and analysis of device positioning in 5G ultra-dense network," in *2019 15th International Wireless Communications Mobile Computing Conference (IWCMC)*, 2019, pp. 1529–1533.

[22] J. A. del Peral-Rosado, J. A. López-Salcedo, G. Seco-Granados, F. Zanier, and M. Crisci, "Achievable localization accuracy of the positioning reference signal of 3GPP LTE," in *2012 International Conference on Localization and GNSS (ICL-GNSS)*, 2012, pp. 1–6.

[23] A. Musa, J. Biagioni, and J. Eriksson, "Trading off accuracy, timeliness, and uplink usage in online GPS tracking," *IEEE Transactions on Mobile Computing*, vol. 15, no. 8, pp. 2124–2136, 2016.

[24] 3GPP RP-193237, "New SID on NR positioning enhancements," Qualcomm Incorporated, Dec. 2019.

[25] Z. Chen, T. Zheng, and J. Luo, "Octopus: A practical and versatile wideband MIMO sensing platform," in *Proceedings of the 27th Annual International Conference on Mobile Computing and Networking (MobiCom '21)*, 2021, pp. 601–614.

[26] Z. Chen, X. Zhang, S. Wang, Y. Xu, J. Xiong, and X. Wang, "Enabling practical large-scale MIMO in wlans with hybrid beamforming," *IEEE/ACM Transactions on Networking*, vol. 29, no. 4, pp. 1605–1619, 2021.

[27] L. Han, R. Liu, Z. Wang, X. Yue, and J. S. Thompson, "Millimeter-wave MIMO-NOMA-based positioning system for internet-of-things applications," *IEEE Internet of Things Journal*, vol. 7, no. 11, pp. 11 068–11 077, 2020.

[28] L. Han, R. Liu, Z. Wang, Q. Liu, Q. Zhu, and J. S. Thompson, "Performance trade-off for integrated communication and data-assisted positioning in MIMO-OFDM system," *China Communications*, vol. 19, no. 11, pp. 129–147, 2022.

[29] Y. Xie, Y. Zhang, J. C. Liando, and M. Li, "Swan: Stitched Wi-Fi antennas," in *Proceedings of the 24th Annual International Conference on Mobile Computing and Networking (MobiCom '18)*, 2018, p. 51–66.

[30] Y. Zhang, W. Sun, Y. Ren, S.-j. Lee, and M. Li, "Channel adapted antenna augmentation for improved Wi-Fi throughput," *IEEE Transactions on Mobile Computing*, pp. 1–14, 2022.

[31] Y. Chan and K. Ho, "A simple and efficient estimator for hyperbolic location," *IEEE Transactions on Signal Processing*, vol. 42, no. 8, pp. 1905–1915, 1994.

[32] Z. Wang, R. Liu, Q. Liu, J. S. Thompson, and M. Kadoch, "Energy-efficient data collection and device positioning in UAV-assisted IoT," *IEEE Internet of Things Journal*, vol. 7, no. 2, pp. 1122–1139, 2020.

[33] Q. Liu, R. Liu, Z. Wang, and J. S. Thompson, "UAV swarm-enabled localization in isolated region: A rigidity-constrained deployment perspective," *IEEE Wireless Communications Letters*, vol. 10, no. 9, pp. 2032–2036, 2021.

[34] Z. Wang, R. Liu, Q. Liu, L. Han, and J. S. Thompson, "Feasibility study of UAV-assisted anti-jamming positioning," *IEEE Transactions on Vehicular Technology*, vol. 70, no. 8, pp. 7718–7733, 2021.

[35] 3GPP TR 38.855, "Study on NR positioning support," v16.0.0, Mar. 2019.

[36] H. Wymeersch, G. Seco-Granados, G. Destino, D. Dardari, and F. Tufvesson, "5G mmwave positioning for vehicular networks," *IEEE Wireless Communications*, vol. 24, no. 6, pp. 80–86, 2017.

[37] J. Zhang, D. Shen, L. Tu, F. Zhang, C. Xu, Y. Wang, C. Tian, X. Li, B. Huang, and Z. Li, "A real-time passenger flow estimation and prediction method for urban bus transit systems," *IEEE Transactions on Intelligent Transportation Systems*, vol. 18, no. 11, pp. 3168–3178, 2017.

[38] X. Lin, J. Bergman, F. Gunnarsson, O. Liberg, S. M. Razavi, H. S. Razaghi, H. Rydn, and Y. Sui, "Positioning for the internet of things: A 3GPP perspective," *IEEE Communications Magazine*, vol. 55, no. 12, pp. 179–185, 2017.

[39] 3GPP R1-1901980, "Further discussion of NR RAT-dependent DL positioning," CATT, Mar. 2019.

[40] R. Hoshyar, M. Shariat, and R. Tafazolli, "Subcarrier and power allocation with multiple power constraints in OFDMA systems," *IEEE Communications Letters*, vol. 14, no. 7, pp. 644–646, 2010.

[41] D. Tian, J. Zhou, Y. Wang, Z. Sheng, X. Duan, and V. C. Leung, "Channel access optimization with adaptive congestion pricing for cognitive vehicular networks: An evolutionary game approach," *IEEE Transactions on Mobile Computing*, vol. 19, no. 4, pp. 803–820, 2020.

[42] J. Zhou, D. Tian, Z. Sheng, X. Duan, and X. Shen, "Distributed task offloading optimization with queueing dynamics in multiagent mobile-edge computing networks," *IEEE Internet of Things Journal*, vol. 8, no. 15, pp. 12 311–12 328, 2021.

[43] X. Liu, H. Zhang, K. Long, A. Nallanathan, and V. C. M. Leung, "Energy efficient user association, resource allocation and caching deployment in fog radio access networks," *IEEE Transactions on Vehicular Technology*, vol. 71, no. 2, pp. 1846–1856, 2022.

[44] 3GPP TS 36.211, "Evolved Universal Terrestrial Radio Access (E-UTRA); Physical channels and modulation," v16.6.0, Jun. 2021.

[45] B. J. Choi, H. Liang, X. Shen, and W. Zhuang, "DCS: Distributed asynchronous clock synchronization in delay tolerant networks," *IEEE Transactions on Parallel and Distributed Systems*, vol. 23, no. 3, pp. 491–504, 2012.

[46] 3GPP TR 36.814, "Evolved Universal Terrestrial Radio Access (E-UTRA); Further advancements for E-UTRA physical layer aspects," v9.2.0, Mar. 2017.

[47] M. Angjelichinoski, D. Denkovski, V. Atanasovski, and L. Gavrilovska, "Cramér–rao lower bounds of RSS-based localization with anchor position uncertainty," *IEEE Transactions on Information Theory*, vol. 61, no. 5, pp. 2807–2834, 2015.

[48] L. L. Scharf and C. Demeure, *Statistical signal processing: Detection, estimation, and time series analysis*. Addison-Wesley Reading, MA, 1991, vol. 63.

[49] F. J. Macwilliams and N. Sloane, "Pseudo-random sequences and arrays," *Proceedings of the IEEE*, vol. 64, no. 12, pp. 1715–1729, 1977.